OFF-CENTER MONOPOLE AND DIPOLE SOURCES IN FLUID-FILLED BOREHOLES

António J. B. Tadeu

Department of Civil Engineering
University of Coimbra
3000 Coimbra, Portugal

M. Nafi Toksöz

Earth Resources Laboratory
Department of Earth, Atmospheric, and Planetary Sciences
Massachusetts Institute of Technology
Cambridge, MA 02139

Eduardo Kausel

Department of Civil and Environmental Engineering
Massachusetts Institute of Technology
Cambridge, MA 02139

ABSTRACT

A variety of seismic testing techniques rely on the use of seismic sources, detectors, or both, placed at some depth below the ground surface; these are often installed within fluid-filled boreholes. The interpretation of the records obtained in the course of such explorations requires a thorough understanding of how waves propagate in the borehole and its immediate vicinity. Depending on the distance between the source and the receiver as well as their placement and orientation relative to the axis of the borehole, it is known that very complex wave patterns may arise. In this paper, analytical-numerical solutions are used to study the wave-field elicited by monopole or dipole sources within a fluid-filled cylindrical cavity drilled through an unbounded homogeneous elastic medium. This model is used to assess the effects of a source-receiver tool, placed in an off-centered and/or tilted position inside the fluid-filled borehole, on the propagation of both axisymmetric and non-axisymmetric wave modes.

INTRODUCTION

Various seismic exploration techniques, such as full waveform acoustic logging, vertical seismic profiling, and cross-hole surveying, use boreholes drilled into the ground to place seismic sources, detectors, or both at some depth below ground. Often, these boreholes are fluid-filled so as to improve the transmission of acoustic energy into the *formation*, i.e., into the surrounding medium. One of the principal obstacles in the interpretation of the recorded signatures is the complexity of the wave patterns that may develop in the borehole environment, particularly when the assembly of source and receivers—the *tool*—is placed in off-axis or tilted positions. In the case of acoustic logs, the position of the tool relative to the axis of the borehole has a crucial effect on the amplitude and times of first arrival of the signals. While the tool is supposed to be held in place on the axis of the borehole by means of bow-type springs and rubber fingers pressing against the formation, these mechanisms may often fail to maintain the tool in perfect alignment. This problem is more pronounced in the case of an inclined or curved borehole, when it is almost impossible to align the sources and receivers along the axis.

A rigorous and detailed examination of the problem described poses formidable computational challenges, which persist even in the case of purely numerical solutions. Thus, to make progress in the analysis, it is necessary to consider idealized conditions that, while still containing the essential features of the full scale problem, are amenable to computation. This paper describes the results obtained with such a model, namely an axisymmetric, fluid-filled cylindrical borehole of infinite length drilled into a homogeneous elastic medium, and subjected to dilatational point sources placed at some point in the fluid. Given the two-dimensional geometry of the model and the three-dimensional characteristics of the source, this problem is commonly said to constitute a two-and-a-half-dimensional problem (or 2-1/2-D for short).

The complexity of the wave patterns recorded at the receivers depends on the relative participation of the many wave propagation modes, or *normal* modes, that may have been excited by the source. This contribution is a function of the distance from the source, the dominant frequency of the pulse, the material characteristics of the formation, and most importantly, the position of the tool relative to the axis of the borehole. When the source is positioned centered on the axis of the borehole, only the axisymmetric normal modes are excited. By contrast, if the source is placed off the borehole axis, additional normal modes having some azimuthal variation are also excited. However, these nonaxisymmetric modes do not contribute to the motions that develop along the axis. Some modes are only excited if the frequency of excitation of the source exceeds certain threshold values referred to as the cutoff frequencies. In addition, the ratio between the shear velocity β_s of the solid medium and the dilatational wave velocity af of the fluid defines two distinct behaviors for wave propagation—when $\beta_s > \alpha_f$ the medium is said to be a *fast formation*; otherwise it is called a *slow formation*.

The interaction of elastic waves with fluid-filled or air-filled cylinders is a problem that has received considerable attention in the literature. Much of the work published

before the last two decades, which focused mainly on dynamic stresses and wave dispersion characteristics and less so on particle motions at a point, was documented in an excellent monograph by Pao and Mow (1973).

The propagation of waves along a borehole boundary was studied nearly half a century ago by Biot (1952), who derived the dispersion equation for guided waves in a borehole, and used it to find the phase and group velocities for these waves. More recently, a number of investigators have addressed the propagation of waves along fluid-filled boreholes from sources aligned with the borehole axis, because of its importance to acoustic logging. Numerical methods have also been used to study the influence on wave amplitude and attenuation by the material characteristics of the formation, by the type of fluid in the borehole, and by the source (e.g., Roever et al., 1974; Tsang and Rader, 1979; Cheng and Toksöz, 1981 ; Kurkjian, 1985; Kurkjian and Chang, 1986; Siggins and Stokes, 1987). The inverse problem of estimating the mechanical properties of the formation has also been the object of research (e.g., Cheng et al., 1987; Paillet and White, 1982), which was later extended to consider the state of fracturing and the presence of damaged zones around the borehole (e.g., Chan and Tsang, 1983; Baker, 1984; Schmitt and Bouchon, 1985; Baker and Winbow, 1988), the effects of spatial variations in the diameter of the borehole (Bouchon and Schmitt, 1989; Randall, 1991a), the presence of anisotropy (e.g., Chan and Tsang , 1983; Schmitt, 1989), and the use of multipole sources (e.g., Kurkjian et al., 1986; Schmitt, 1989). Randall (1991b) also studied the multipole acoustic log in the non-axisymmetric borehole using the 2-1/2-D finite difference method.

The interaction of elastic plane waves incident upon a fluid- or air-filled borehole has been investigated in the context of vertical profiling and cross-hole surveying. Blair (1984) considered the case of a P-wave normally incident to the borehole axis, while Schoenberg (1986) studied the problem of plane compressional or shear waves impinging at arbitrary angles on the fluid borehole. He provided explicit formulas that are valid only for low frequencies. This problem was taken up again by Lovell and Hornby (1990), who developed expressions valid over all frequencies and incidence angles. However, both Schoenberg and Lovell and Hornby provided results for the pressure only at the center of the fluid-filled borehole. A simplifying feature of the pressure at points on the axis is that this quantity depends only on the axisymmetric part of the solution. By contrast, the influence of an off-centered or tilted tool has received comparatively little attention. Simple approximate modeling techniques were used by Willis et al. (1983) to estimate the sensitivity of the full acoustic waveforms to tool positioning.

In the remainder of this paper, we address this issue once more and compute the wavefield and motions elicited by monopole or dipole sources placed in off-centered positions. We first compute the solution for a wide range of frequencies and wavenumbers, which are then used to obtain time series by means of (fast) inverse Fourier transforms into space-time. Finally, we present a set of synthetic waveforms for monopole and dipole sources placed in off-centered positions in a fast formation.

Because of the cylindrical geometry of this problem, we can use the separation

of variables and express the solution at each frequency in terms of waves with varying wavenumber k_z (with z being the borehole axis), which we subsequently Fourier-transform into the spatial domain. We cast this wavenumber transform in discrete form by considering an infinite number of virtual point sources equally spaced along the z axis and at a sufficient distance from each other to avoid spatial contamination (Bouchon and Aki, 1977). In addition, we carry out the analysis using complex frequencies, shifting downward—in the complex plane—the frequency axis in order to remove the singularities on (or near) the axis, and to minimize the influence of the neighboring fictitious sources (Phinney, 1965).

FORMULATION OF THE PROBLEM

Since the methods used for solving the wave scattering problem, such as the one considered in this paper, are well-known, it suffices to present a sketch of the formulation.

Consider a spatially uniform elastic medium of infinite extent, having a cylindrical cavity filled with an inviscid fluid (Figure 1). Decomposing as usual the homogeneous wave equations for elastic media by means of the now classical dilatational potential ϕ and shear potentials ψ, χ, one is led to the three scalar wave equations in these potentials, with associated wave propagation velocities α, β, and β, respectively. For an harmonic dilatational point source at an off-center position $(x_0, 0, 0)$ in the fluid or solid that is oscillating with a frequency ω, the scalar wave equations go over into three Helmholtz equations whose solution can be expressed in terms of the single dilatational potential for the *incident* waves together with the set of potentials for *scattered* waves in both media.

Incident Field (or Free-Field)

The incident dilatational potential is given by the expression

$$\phi_{inc} = \frac{Ae^{i\frac{\omega}{\alpha}(\alpha t - \sqrt{(x-x_0)^2+y^2+z^2})}}{\sqrt{(x-x_0)^2+y^2+z^2}} \tag{1}$$

in which the subscript *inc* denotes the incident field, A is the wave amplitude, α is the acoustic (dilatational) wave velocity *of the medium containing the source*, and $i = \sqrt{-1}$.

Defining the effective wavenumbers

$$k_\alpha = \sqrt{\frac{\omega^2}{\alpha^2} - k_z^2}, \quad \text{Im } k_\alpha < 0$$

$$k_\beta = \sqrt{\frac{\omega^2}{\beta^2} - k_z^2}, \quad \text{Im } k_\beta < 0 \tag{2}$$

by means of the axial wavenumber k_z, the frequency of excitation ω, and the wave velocities α, β, and Fourier-transforming Eq. 1 in the z direction, one obtains

$$\phi_{inc}(\omega, x, y, k_z) = \frac{-iA}{2} H_0^{(2)}(k_\alpha \sqrt{(x-x_0)^2 + y^2}) \tag{3}$$

in which the $H_n^{(2)}(\ldots)$ are second Hankel functions of order n.

Equation 3 poses a difficulty, however, because it expresses the incident field in terms of waves centered at the source point $(x_0, 0, 0)$, and not at the axis of the borehole. This difficulty can be overcome by expressing the incident potential in terms of waves centered at the origin, which can be achieved by recourse to Graf's addition theorem (Watson, 1980, p. 361), leading to the expressions (in cylindrical coordinates):

$$\phi_{inc}(\omega, r, \theta, k_z) = -iA \sum_{n=0}^{\infty} (-1)^n \epsilon_n H_0^{(2)}(k_\alpha r_0) J_n(k_\alpha r) \cos n\theta \quad \text{when } r < r_0 \quad (4)$$

$$\phi_{inc}(\omega, r, \theta, k_z) = -iA \sum_{n=0}^{\infty} (-1)^n \epsilon_n H_0^{(2)}(k_\alpha r) J_n(k_\alpha r_0) \cos n\theta \quad \text{when } r > r_0 \quad (5)$$

in which the $J_n^{(2)}(\ldots)$ are Bessel functions of order n, θ is the azimuth, and

$$\epsilon_n = \begin{cases} \frac{1}{2} \text{ if } n=0 \\ 1 \text{ if } n \neq 0 \end{cases}$$

$$r = \sqrt{x^2 + y^2} = \text{radial distance to the receiver}$$

$$r_0 = \sqrt{x_0^2} = |x_0| = \text{radial distance to the source}$$

$$\cos \theta = x/r, \quad \sin \theta = y/r \quad (6)$$

Scattered Field in the Exterior Region (Solid)

In the frequency-axial-wavenumber domain, the scattered field in the *exterior* region (the solid formation) can be expressed in a form similar to that of the incident field, namely

$$\phi_{sca}^s(\omega, r, \theta, k_z) = \sum_{n=0}^{\infty} A_n H_n^{(2)}(k_{\alpha s} r) \cos n\theta$$

$$\psi_{sca}^s(\omega, r, \theta, k_z) = \sum_{n=0}^{\infty} B_n H_n^{(2)}(k_{\beta s} r) \sin n\theta$$

$$\chi_{sca}^s(\omega, r, \theta, k_z) = \sum_{n=0}^{\infty} C_n H_n^{(2)}(k_{\beta s} r) \cos n\theta \quad (7)$$

in which the subscript *sca* denotes the scattered field, A_n, B_n, and C_n are as yet unknown coefficients to be determined from appropriate boundary conditions, and the additional index s indicates that the wave velocities of the *solid* must be used. Together with an implicit factor $\exp i(\omega t - k_z z)$, the second Hankel functions in Eqs. 6 represent diverging or outgoing cylindrical waves. Because of the symmetry of the source with respect to the x-z plane, Eqs. 6 involve either the $\cos n\theta$ or $\sin n\theta$ terms, but not both simultaneously.

Scattered Field in the Interior Region (Fluid)

If the source is *outside* the borehole (i.e., within the formation), the scattered (or refracted) field in the fluid consists of standing waves, which can be expressed as:

$$\phi_{sca}^{f}(\omega, r, \theta, k_z) = \sum_{n=0}^{\infty} D_n J_n(k_{\alpha f} r) \cos n\theta \tag{8}$$

with the index f identifying the fluid.

By contrast, if the source is *inside* the borehole (i.e., in the fluid), the scattered field is given by

$$\phi_{sca}^{f}(\omega, r, \theta, k_z) = \sum_{n=0}^{\infty} D_n H_0^{(2)}(k_\alpha r_0) J_n(k_\alpha r) \cos n\theta \quad \text{when } r < r_0$$

$$\phi_{sca}^{f}(\omega, r, \theta, k_z) = \sum_{n=0}^{\infty} D_n H_0^{(2)}(k_\alpha r) J_n(k_\alpha r_0) \cos n\theta \quad \text{when } r > r_0 \tag{9}$$

Displacement Field

The unknown constants A_n, B_n, C_n, D_n in Eqs. 6–8 are obtained by imposing the continuity of displacements and stresses at the interface between the solid and the fluid, namely $u_r^s = u_r^f$, $\sigma_{rr}^s = \sigma_{rr}^f$, and $\sigma_{r\theta}^s = \sigma_{rz}^s = 0$. Notice that since we have assumed an inviscid fluid, the tangential displacements at the boundary of the solid (i.e., u_θ^s, u_z^s) may be different from those in the fluid (i.e., u_θ^f, u_z^f). The imposition of the four stated boundary conditions for each summation index n leads then to a system of four equations in the four unknown constants. While this procedure is straightforward, the details are somewhat messy, and are best left out.

Having obtained the constants, we may compute the motions associated with the scattered field by means of the well-known equations relating potentials and displacements. In essence, this requires the consideration of Eqs. 6 as well as 7 or 8—depending on whether the source is outside or inside the borehole—and taking partial derivatives to go over from potentials to displacements. After carrying out this procedure, one obtains expressions for the scattered field in the solid and fluid of the form:

$$u_r(\omega, r, \theta, k_z) = \sum_{n=0}^{\infty} f_n(r) \cos n\theta$$

$$u_\theta(\omega, r, \theta, k_z) = \sum_{n=0}^{\infty} g_n(r) \sin n\theta$$

$$u_z(\omega, r, \theta, k_z) = \sum_{n=0}^{\infty} h_n(r) \cos n\theta \tag{10}$$

in which the functions f_n, g_n, h_n are given by:

Solid:

$$
\begin{aligned}
f_n(r) &= \left[\frac{n}{r}H_n^{(2)}(k_{\alpha s}r) - k_{\alpha s}H_{n+1}^{(2)}(k_{\alpha s}r)\right]A_n + \frac{n}{r}H_n^{(2)}(k_{\beta s}r)B_n - ik_z\left[\frac{n}{r}H_n^{(2)}(k_{\beta s}r)\right. \\
&\quad \left. -k_{\beta s}H_{n+1}^{(2)}(k_{\beta s}r)\right]C_n \\
g_n(r) &= -\frac{n}{r}H_n^{(2)}(k_{\alpha s}r)A_n + \left[\frac{n}{r}H_n^{(2)}(k_{\beta s}r) - k_{\beta s}H_{n+1}^{(2)}k_{\beta s}r)\right]B_n + ik_z\frac{n}{r}H_n^{(2)}(k_{\beta s}r)C_n \\
h_n(r) &= -ik_zH_n^{(2)}(k_{\alpha s}r)A_n + k_{\beta s}^2H_n^{(2)}(k_{\beta s}r)B_n
\end{aligned}
\tag{11}
$$

Fluid:

$$
\begin{aligned}
f_n(r) &= \left[\frac{n}{r}J_n(k_{\alpha f}r) - k_{\alpha f}J_{n+1}(k_{\alpha f}r)\right]D_n \\
g_n(r) &= -\frac{n}{r}J_n(k_{\alpha f}r)D_n \\
h_n(r) &= -ik_zJ_n(k_{\alpha f}r)D_n
\end{aligned}
\tag{12}
$$

From these equations, it follows that on the axis of the borehole, only the $n=0$ terms survive, and we recover the expressions derived earlier by Lovell and Hornby (1990). On the other hand, at points away from the axis, the displacements are also a function of the non-axisymmetric terms with $n>0$. Finally, the incident field—obtained from Eq. 4a or 4b by partial differentiation must be added to Eqs. 9 for the medium containing the source so as to obtain the total field in the k_z wavenumber domain.

Displacements in Space-Time

The displacements in the spatial-temporal domain are obtained by a numerical fast Fourier transform in k_z and, considering a source whose temporal variation is given by a Ricker wavelet. This wavelet form is chosen because it decays rapidly in both time and frequency; this not only reduces the computational effort, but allows easier interpretations of the computed time series and synthetic waveforms.

As stated before, the Fourier transformations are achieved by discrete summations over wavenumbers and frequencies, which is mathematically equivalent to adding periodic sources at spatial intervals $L = 2\pi/\Delta k_z$ (in the z-axis) and temporal intervals $T = 2\pi\Delta\omega$, with Δk_z and $\Delta\omega$ being the wavenumber and frequency steps, respectively (Bouchon and Aki, 1977). The spatial separation L must be large enough if one is to avoid contamination of the response by the periodic sources. In other words, the contribution to the response by the fictitious sources must be guaranteed to occur at times later than T. This goal can also be aided substantially by slightly shifting the frequency axis downward, that is, by considering complex frequencies with a small imaginary part of the form $\omega_c = \omega - i\eta$ (with $\eta \approx \Delta\omega$). This technique results in a large attenuation or virtual elimination of the periodic sources (Phinney, 1965). In the time domain,

this shift is later taken into account by applying an exponential window $\exp \eta t$ to the response (Kausel, 1992).

Dipole Sources

In a fluid medium, a dipole source—and all multipole sources of higher order, such as the quadrupole source—can be built from collections of monopole sources. In particular, a dipole source is constructed from two point sources of opposite sign and weight 1/2, placed close together in the same horizontal plane (Kraus and Carver, 1973; Kurkjian *et al.*, 1986), as shown in Figure 2.

DISPERSION OF WAVES IN A FLUID-FILLED BOREHOLE

Of the various waves propagating along the boundary of a fluid-filled borehole, two are non-dispersive body waves, namely the dilatational (P) and shear (S) waves. When the source is within the borehole, the waves begin as dilatational waves in the fluid. As they reach the borehole boundary, they are critically refracted into the formation as P or S waves, which are in turn refracted back into the fluid as P waves. In addition, there are various types of guided waves—the normal modes—propagating along the interface between the fluid and solid. As stated previously, when the source is positioned on the axis of the borehole, only the axisymmetric modes are excited. By contrast, additional modes with some azimuthal variation are excited when the source is placed away from the axis, but these modes do not contribute to the pressures recorded at receivers positioned on the axis. On the other hand, certain modes are excited only if the frequency of excitation of the source exceeds the cutoff (or resonant) frequencies of the borehole.

The dispersion characteristics of the normal modes can be obtained by solving an eigenvalue problem in the constants A_n, B_n, C_n, D_n in the absence of an incident field (i.e., with $A = 0$). The associated eigenvalues k_z lead in turn to the phase and group velocities of the normal modes. While an infinite (but countable) number of modes exist, only those with low modal order contribute significantly to the response.

The normal modes depend strongly on the ratio β_s/α_f between the shear wave velocity in the solid medium and the dilatational wave velocity in the fluid. If this ratio is less than one (i.e., a slow formation), proper normal modes do not exist because any waves propagating in the fluid will radiate and lose their energy as shear waves in the solid. However, one can still find in this case modes with a complex wavenumber (referred to as leaky modes) which attenuate rapidly as they propagate. On the other hand, if the stated ratio is larger than one (a fast formation), energy may remain trapped in the borehole and normal modes do exist; in addition, there may also be leaky modes. In general, the amplitude of the normal modes in the formation decays exponentially with distance to the borehole. Thus, the phase and group velocities of all normal modes must be smaller than the shear wave velocity in the formation, except of course for the leaky modes.

Off-Center Monopole and Dipole Sources in Fluid-Filled Boreholes

To focus our ideas, let us revisit the example of a fast formation studied by Ellefsen (1990):

$$\alpha_s = 4208 \text{ m/s} \qquad\qquad \beta_s = 2656 \text{ m/s} \quad \rho_s = 2140 \text{ Kg/m}^3$$
$$\alpha_f = 1500 \text{ m/s} \qquad\qquad\qquad\qquad\qquad \rho_f = 1000 \text{ Kg/m}^3 \qquad (13)$$
$$a = 0.1016 \text{ m} = \text{radius of borehole}$$

Figures 3 and 4 give, respectively, the phase velocities and group velocities for the lowest order normal modes as calculated by Ellefsen (1990). In these figures, the modes are identified by a pair of numbers. The first number in the pair is the azimuthal order, which indicates the variation of the mode with the azimuth, while the second is the radial order giving the variation of the mode with radial distance. The first axisymmetric mode is the *tube wave* or Stoneley wave. The tube wave exists at all frequencies, and is associated in Figures 3 and 4 with the pair (0,0). This wave exhibits a slight dispersion and its energy is usually highest at low frequencies. Its phase and group velocities are below the dilatational velocity of the fluid.

The second axisymmetric mode is the *pseudo-Rayleigh wave* [(0,1)], which has in this case a cutoff frequency of 8 kHz. At this cutoff frequency, the mode reaches its highest phase velocity, namely the shear wave velocity of the solid. As the frequency of the waves increases, the phase velocity of the mode approaches asymptotically—from above—the fluid velocity. On the other hand, the group velocity is less than the shear wave velocity of the solid at the low-frequency cutoff. From this point on, it decreases rapidly with frequency, reaches a minimum associated with Airy waves, and approaches thereafter from below the fluid velocity. Thus, the pseudo-Rayleigh wave is highly dispersive.

There is also an infinite number of higher order pseudo-Raleigh waves [(0,2),(0,3),..] which have correspondingly higher cutoff frequencies. Within the fluid cylinder, these waves are oscillatory in nature and decay with distance from the axis. The amplitude of the first mode, for example, has a zero value at a point located at (approximately) 2/3 of the distance between the axis and the borehole wall.

The first mode with azimuthal variation is the *flexural wave* [(1,0)], which exists at all frequencies. The fluid pressure for this mode varies as the cosine or sine of the azimuthal angle. As can be seen in Figs. 3 and 4, this mode is highly dispersive. Higher flexural modes also exist, such as the [(1,1), (1,2)] modes shown.

The second azimuthal modes, which vary as $\cos 2\theta$ or $\sin 2\theta$, are referred to as the *screw waves*. The fundamental screw wave [2,0] has a cutoff frequency of approximately 6 kHz. Again, an infinite number of higher order modes exist [(2,1),(2,2)..].

Higher order normal modes [(n, m)] for $m, n > 2$ which vary as $\cos n\theta$ or $\sin n\theta$ also exist, but these have no common name.

Synthetic Waveforms

We next apply the methodology described to study wave signatures in the borehole considered in the previous section when excited by monopole and dipole sources in the

fluid medium placed close to the wall, as depicted in Figure 5. Also illustrated in this figure are the receivers, set at a distance of 20 m from the source in the positions shown.

We perform our computations in the frequency range from zero to 20480 Hz, with a frequency increment of 40 Hz; thus, the total time duration of the analysis is T=1/40 =0.025s = 25ms. This implies, in turn, that the spatial period cannot be less than $L = 2T\alpha_s$ =2x0.025x4208 = 210.4m. We choose $\eta = 0.7\Delta\omega$ as the imaginary part for the angular frequency, so as to attenuate the wraparound by a factor of $\exp 0.7\Delta\omega T = 81$ (i.e., 38 dB). The source is a Ricker wavelet pulse with a characteristic frequency of 7500 Hz. In all cases, the computed wave fields refer to pressure when the source is a monopole, and to radial displacements when the source is a dipole. Also, all plots are normalized with respect to their own maxima.

Monopole Source

In a fast formation, the disturbance begins as a dilatational wave in the borehole fluid which is critically refracted into the formation as P and S waves; these are then refracted back into the fluid as a dilatational wave. After the P-wave arrival, the response is marked by a dense ringing called the leaky or PL mode. The arrows in Figure 6 point to the arrival of the P and S body waves. Since at the scale of the plots they cannot be easily identified, we blow up the early part of the graph in an inset so as to show these arrivals. Notice the ringing of the packed leaky mode occurring between the P and S waves.

As we stated before, a source placed off the axis excites both axisymmetric and non-axisymmetric modes, but only the former contribute to the pressure on the axis. Hence, at receiver #1 (Figure 6a), only the body waves, the Stoneley waves, and the pseudo-Rayleigh waves are observed. The response there is similar to the one that would be generated by a source on the axis (not shown), except that the amplitudes of the response are now lower, and the importance of the Stoneley wave higher than for centered sources.

If we consider the group velocities of the various modes and the amplitude of the pressures obtained, we can visually separate the modes. For example, Figure 4 indicates that the group velocity of bending waves is higher than that of screw waves, which in turn is higher than for pseudo-Rayleigh waves.

We also observe that the signatures at receivers 4 and 7 are not affected by flexural waves, because the bending mode has zero amplitude on the neutral axis, which is the horizontal plane through the axis that is perpendicular to the line connecting the center with the source. Hence, after the passage of the Stoneley wave, the signatures on the neutral axis experience a substantial drop in amplitude (Figures 6d–g). This drop, however, is not observed for receivers 2, 3, 5, 6 located away from the neutral axis (Figures 6b,c,e,f). Indeed, receivers 5 and 6 that are farthest from the neutral axis exhibit the largest increases in pressure, which are clearly due to the flexural mode.

Trailing behind the flexural waves is a set of pulses associated with the screw mode. We verify that their contribution to the pressure at receivers 3 and 6, which lie in 45

degree planes, is very small, as theory would predict.

After the screw waves follow the first order pseudo-Rayleigh waves. Their contribution to the pressure signatures grows from receivers 4 to 7, from 3 to 6, and from 2 to 5, because these waves have near zero amplitude at the 2/3 radial distance, as previously mentioned.

If we inspect the response at the receivers closely, we can also detect some of the higher modes, such as mode (3,0). The pressure associated with this mode varies as either $\cos 3\theta$ or $\sin 3\theta$, which gives zero on the neutral axis and maximum value at the position of receiver 5. At the same time, the contribution of this mode decreases toward the axis and vanishes completely.

Dipole Source

Figure 7 shows the synthetic waveforms for a dipole source. Once more, since the first passage of the body waves is not obvious in these plots, we have added arrows to indicate their arrival. Some of the features in these plots resemble those for the monopole source. However, the shear mode is now stronger, whereas no Stoneley (or tube) wave is detectable. Note also that the amplitudes of the waves in the fluid oscillate and decay towards the wall of the borehole. On the other hand, the participation of the higher order modes is not very different from before.

CONCLUSIONS

We have used a method based on discrete integration over wavenumbers and frequencies to compute the wave signatures associated with monopole and dipole dilatational sources placed in off-centered positions in a fluid-filled cylindrical borehole surrounded by a fast formation. Our discretization of the wavenumber-frequency integral transform is mathematically equivalent to a periodic sequence of sources parallel to the axis of the borehole that are also periodic in time. We have removed the effects of these periodicities by recourse to complex frequencies (i.e., by a numerical implementation of the Bromwich transform, or inverse Laplace transform).

The synthetic signatures we obtained agree well with theoretical considerations based on wave arrival and content.

ACKNOWLEDGMENTS

REFERENCES

Abramowitz, M. and I.A. Stegun, 1972, *Handbook of Mathematical Functions*, U.S. Department of Commerce, Tenth Printing.

Baker, L. J., 1984, The effect of the invaded zone on full wavetrain acoustic logging, *Geophysics, 49,* 796–809.

Baker, L. J. and G. A. Winbow, 1988, Multipole P-wave logging in formations altered by drilling, *Geophysics, 53,* 1207-1218.

Biot, M. A., 1952, Propagation of elastic waves in cylindrical bore containing a fluid, *J. Appl. Phys., 23,* 997-1005.

Blair, D. P., 1984, Rise times of attenuated seismic pulses detected in both empty and fluid-filled cylindrical boreholes, *Geophysics 49,* 398-410.

Bouchon, M. and D. P. Schmitt, 1989, The full-wave acoustic logging in an irregular borehole, *Geophysics, 54,* 758-765.

Bouchon, M. and Keiti Aki, 1977, Discrete wave-number representation of seismic source wavefields, *Bull. Seism. Soc. Am., 67,* 259-277.

Chan, A. K. and L. Tsang, 1983, Propagation of acoustic waves in a fluid-filled borehole surrounded by a concentrically layered transversely isotropic formation, *J. Acoust. Soc. Am., 74,* 1605-1616, 1983.

Cheng, C. H. and M. N. Toksöz, 1981, Elastic wave propagation in a fluid-filled borehole and synthetic acoustic logs, *Geophysics, 46,* 1042-1053.

Cheng, C. H., J. Zhang and D. R. Burns, 1987, Effects of in-situ permeability on the propagation of stoneley (tube) waves in a borehole, *Geophysics, 52,* 1279–1289.

Ellefsen, K. J., 1990, Elastic wave propagation along a borehole in an anisotropic medium, Ph.D., Department of Earth and Planetary Sciences, M.I.T.

Kausel, E., 1992, Frequency domain analysis of undamped systems, *Journal of Engineering Mechanics, ASCE, 118,* 721-734.

Kraus, J. D., and Carver, K. R., 1973, *Electromagnetics*, McGraw-Hill Book Co., pp. 37–39.

Kurkjian, A. L., 1985, Numerical computation of individual far-field arrivals excited by an acoustic source in a borehole, *Geophysics, 50,* 852–856.

Kurkjian, A. L., 1986, Theoretical far-field radiation from a low-frequency horizontal acoustic point force in a vertical borehole, *Geophysics, 51,* 930-939.

Kurkjian, A. L. and Shu-Kong Chang, 1986, Acoustic multipole sources in fluid-filled boreholes, *Geophysics, 51,* 148-163.

Lovell, J. R. and B. E. Hornby, 1990, Borehole coupling at sonic frequencies, *Geophysics, 55,* 806-814.

Paillet, F. L. and J. E. White, 1982, Acoustic modes of propagation in the borehole and their relationship to rock properties, *Geophysics, 47,* 1215-1228.

Pao, Y. H. and C. C. Mow, 1973, *Diffraction of Elastic Waves and Dynamic Stress Concentrations*, Rand Corporation.

Phinney, R.A., 1965, Theoretical calculation of the spectrum of first arrivals in layered elastic medium, *J. Geophys. Res.*, 70, 5107–5123.

Randall, C.T., 1991a, Modes of noncircular fluid-filled boreholes in elastic formation, *J. Acoust. Soc. Am., 89*, 1002–1016.

Randall, C.T., 1991b, Multipole acoustic waveforms in nonaxisymmetric boreholes and formations, *J. Acoust. Soc. Am., 90*, 1620–1631.

Roever, W. L., J. H. Rosenbaum, and T. F. Vining, 1974, Acoustic waves from an impulsive source in a fluid-filled borehole, *J. Acoust. Soc. Am., 55*, 1144-1157.

Schoenberg, M., 1986, Fluid and solid motion in the neighborhood of a fluid-filled borehole due to the passage of a low frequency elastic plane wave, *Geophysics, 51*, 1191-1205.

Schmitt, D.P., 1989, Acoustic multipole logging in transversely isotropic poroelastic formations, *J. Acoust. Soc. Am., 86*, 2397–2421.

Schmitt, D. P. and M. Bouchon, 1985, Full-wave acoustic logging: synthetic microseismograms and frequency-wavenumber analysis, *Geophysics, 50*, 1756-1778.

Siggins, A. F. and A. N. Stokes, 1987, Circumferential propagation of elastic waves on boreholes and cylindrical cavities, *Geophysics, 52*, 514–529.

Tadeu, Antonio J. B., 1992, Modelling and seismic imaging of buried structures, Ph.D., M.I.T., Department of Civil Engineering, Cambridge, Massachusetts.

Tsang , L. and D. Rader, 1979, Numerical evaluation of the transient acoustic waveform due to a point source in a fluid-filled borehole, *Geophysics, 44*, 1706-1720.

Watson, G. N., 1980, *A Treatise on the Theory of Bessel Functions*, Cambridge University Press, Second Edition.

Willis, M. E., M. N. Toksöz, and C.H. Cheng, 1983, Approximative effects of off-center acoustic sondes and elliptic boreholes upon full waveform logs, Full Waveform Acoustic Logging Consortium, Annual Report, Earth Resources Laboratory, Massachusetts Institute of Technology.
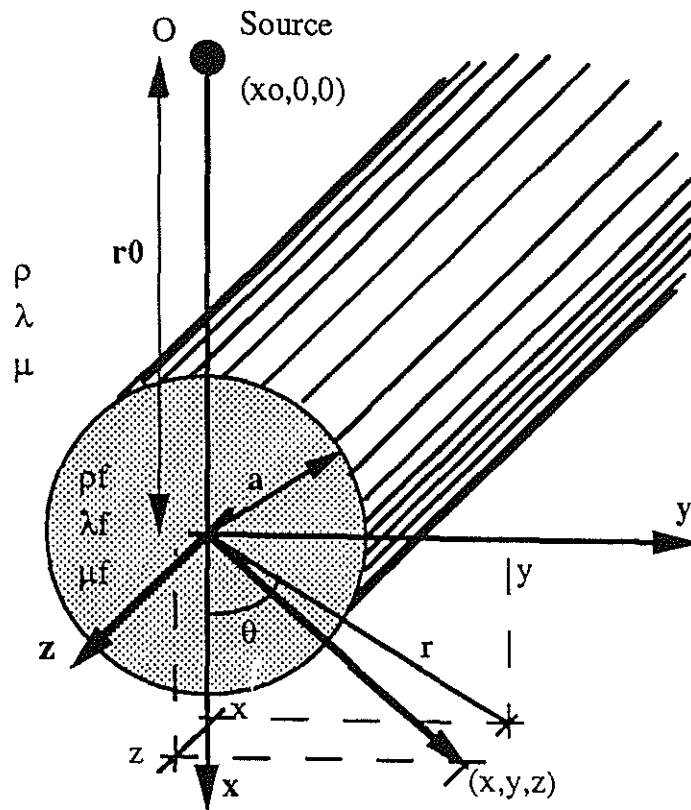
Figure 1: Cylindrical cavity in an unbounded medium.
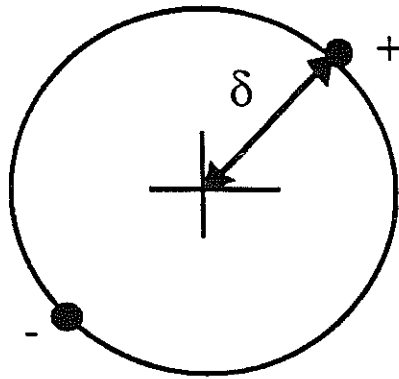
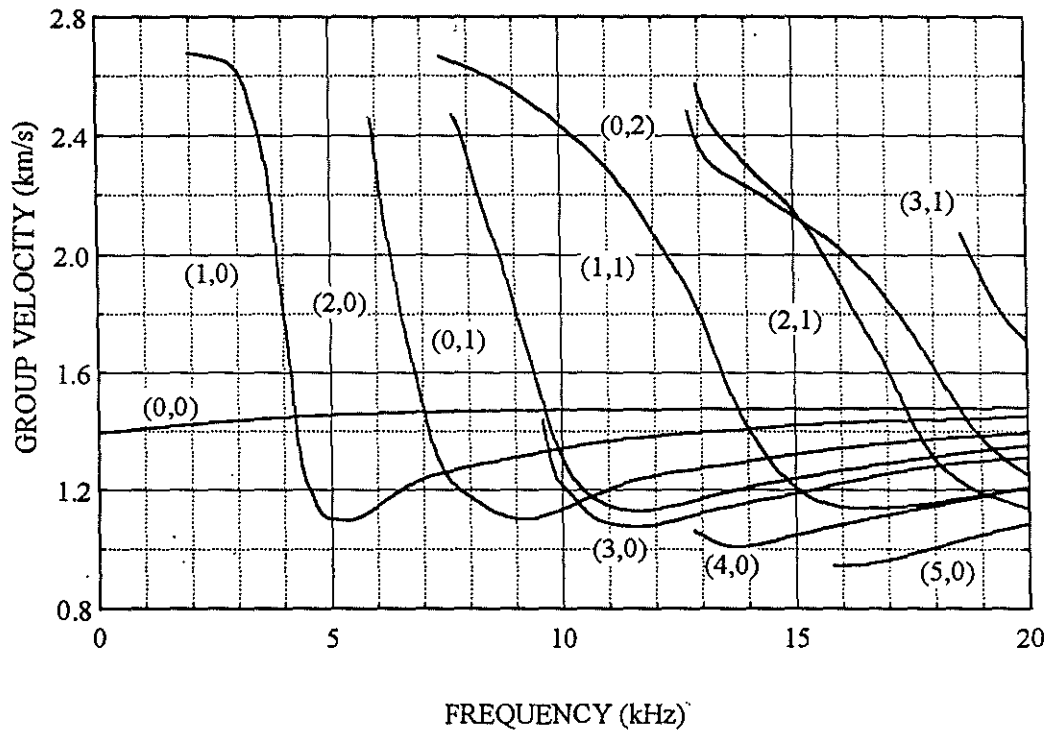Figure 2: Dipole source.
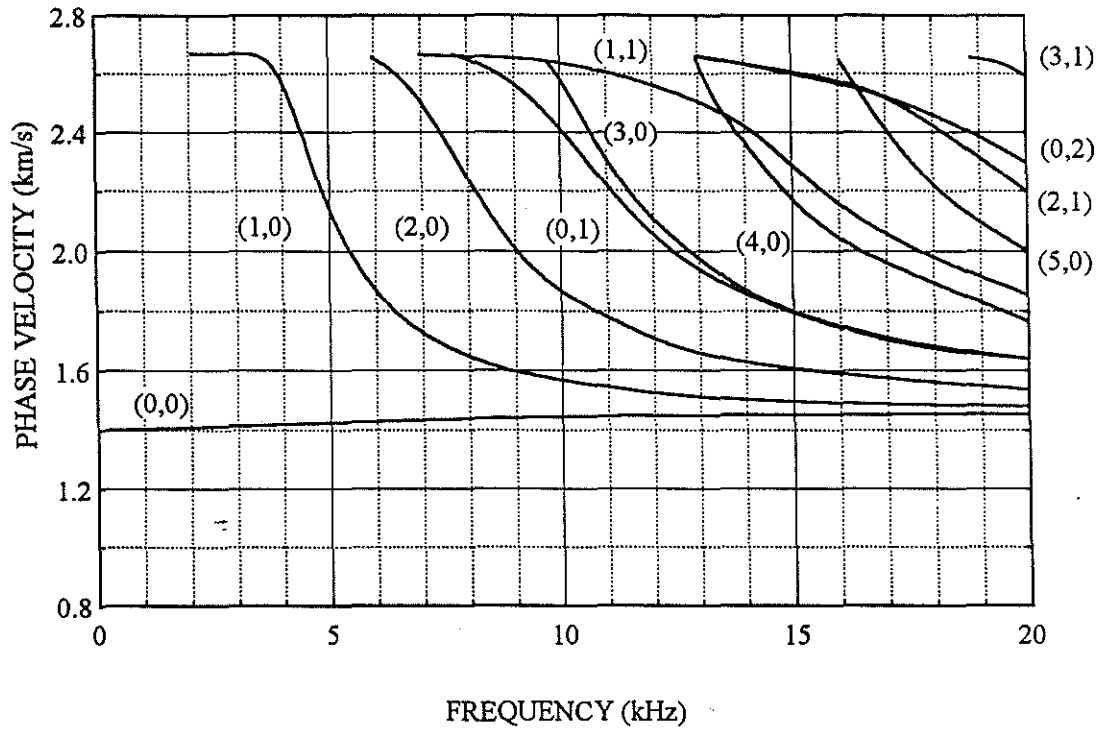
Figure 3: Phase velocities for the lowest order normal modes.

Figure 4: Group velocities for the lowest order normal modes.
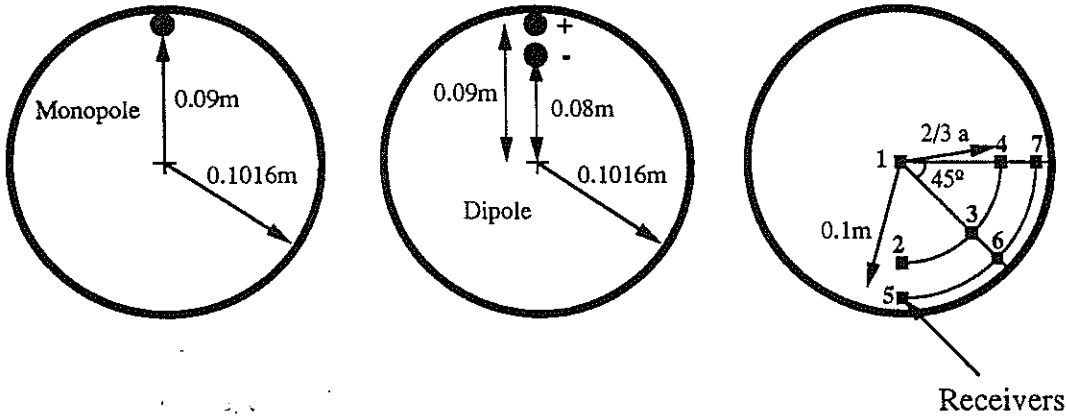
Figure 5: Position of source and receivers.

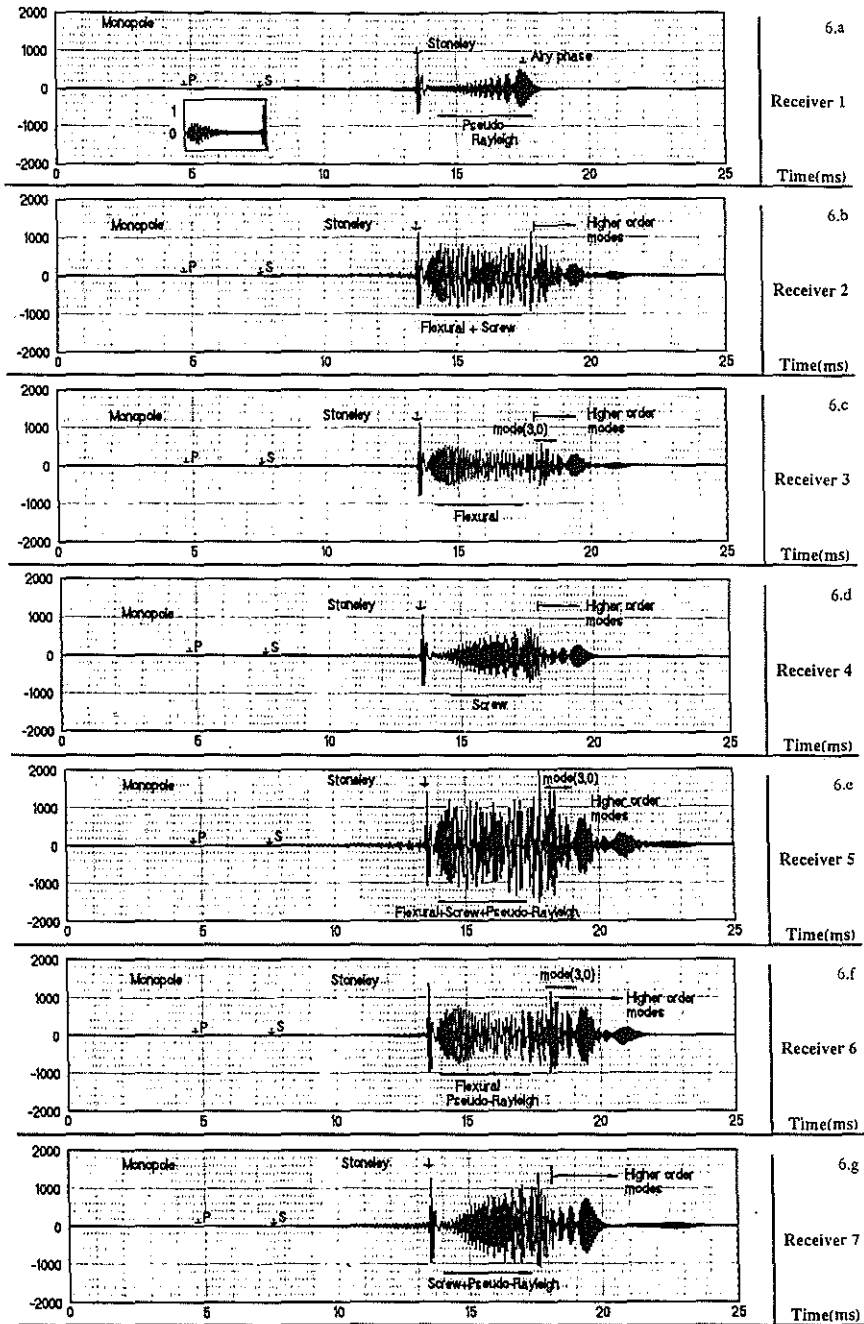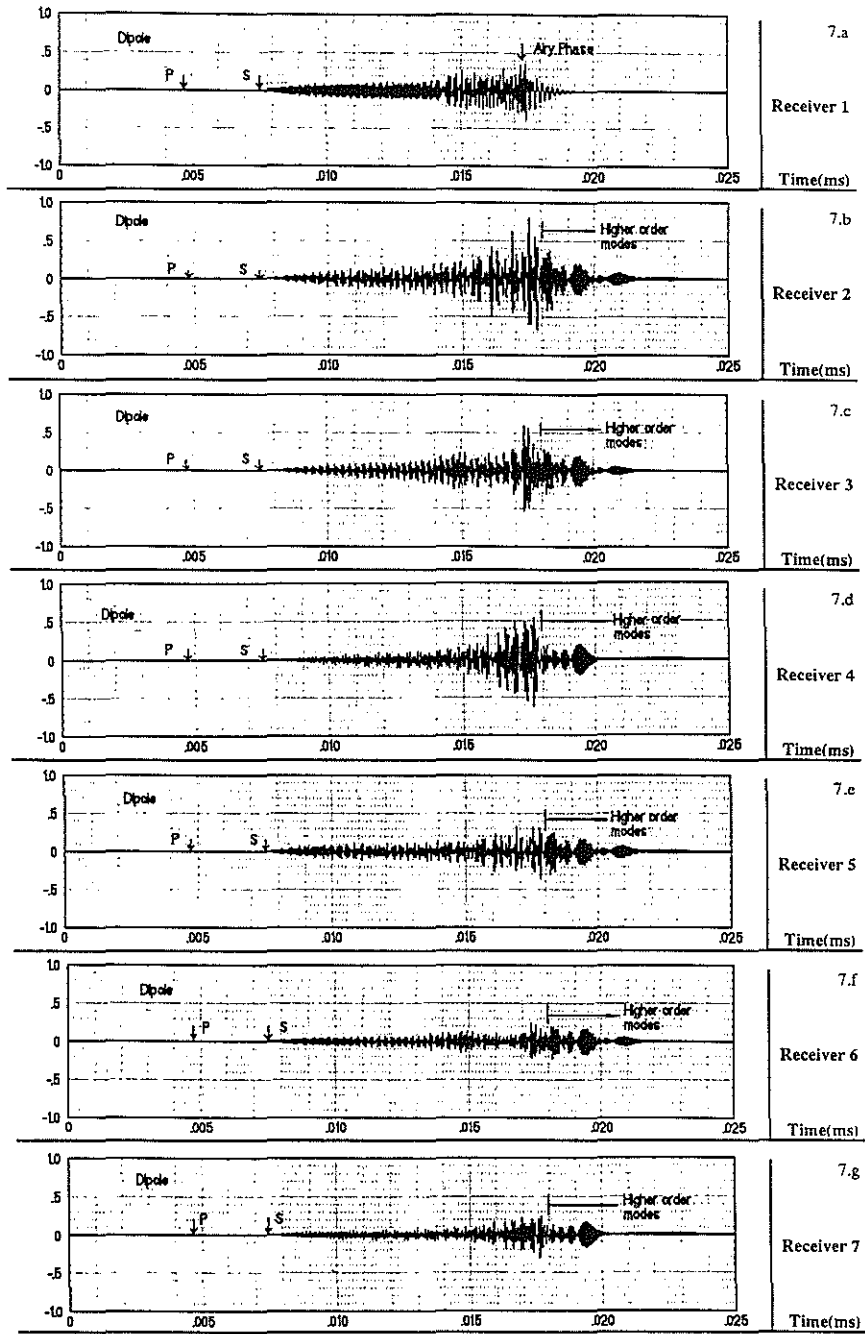Figure 6: Pressures at receivers #1, #2, #3, #4, #5, #6, and #7.

Figure 7: Displacements at receivers #1, #2, #3, #4, #5, #6, and #7.